

Hopf characterization of two-dimensional Floquet topological insulators

F. Nur Ünal,^{1,*} André Eckardt,^{1,†} and Robert-Jan Slager^{2,‡}

¹*Max-Planck-Institut für Physik komplexer Systeme, Nöthnitzer Straße 38, 01187 Dresden, Germany*

²*Department of Physics, Harvard University, Cambridge, MA 02138*

(Dated: December 15, 2024)

We present a topological characterization of time-periodically driven two-band models in $2 + 1$ dimensions as Hopf insulators. The intrinsic periodicity of the Floquet system with respect to both time and the underlying two-dimensional momentum space constitutes a map from a three dimensional torus to the Bloch sphere. As a result, we find that the driven system can be understood by appealing to a Hopf map that is directly constructed from the micromotion of the drive. Previously found winding numbers are shown to correspond to Hopf invariants, which are associated with linking numbers describing the topology of knots in three dimensions. Moreover, after being cast as a Hopf insulator, not only the Chern numbers, but also the winding numbers of the Floquet topological insulator become accessible in experiments as linking numbers. We exploit this description to propose a feasible scheme for measuring the complete set of their Floquet topological invariants in optical lattices.

Introduction – With the advent of topological insulators [1, 2], the past decades have witnessed a rekindling of interest in band theory. The interplay between symmetry and topology has led to the prediction and observation of many novel gapped and semi-metallic electronic topological phases. While the topological classification of such free-fermion systems is by now rather well understood [3–11], notions and invariants such as Chern numbers have increasingly found generalizations in the context of periodically driven quantum systems [12–15]. A striking result was found recently also for quenched systems [16–20], where it was shown, by using a composition map amounting to a Hopf map, that the Chern number can be directly understood as a linking number. Such out-of-equilibrium topological characterizations are not only intriguing from a theoretical perspective, but are also increasingly finding their way to experimental settings of ultracold atoms in Floquet-engineered optical lattices, where the Berry curvature and Chern numbers of Bloch bands have been measured [17, 21–28].

Nonetheless, while the topological characterization of non-equilibrium periodically driven lattice systems in two dimensions was established theoretically, the winding numbers characterizing these systems have not been observed directly in experiments so far, whereas the associated anomalous edge states were probed in photonic systems [29–33]. Here we reveal that the full topological characterization of the system can be achieved via a simple but universal scheme that involves Hopf maps. In particular, the winding numbers are shown to directly correspond to Hopf invariants. In contrast to the symmetry protected topological phases, topology of Hopf insulators relate to the topology of knots formed in three dimensions under the Hopf map. That is, whereas symmetry protected topological band theory involves K-theory and hence is stable to the addition of higher bands, Hopf insulators coincide with a Hopf map by virtue of being a two band model. Specifically, the Grassmannian target

manifold $Gr(m, m + n) = Gr(1, 2)$ is topologically the same as a sphere S^2 . Several proposals involving three-dimensional crystals [34–37] and dipolar gases [38] have been theoretically studied and proposed as platforms to identify this novel topologically insulating state, however, with no luck in an experimental observation so far. In this paper, we consider a two-band model in two dimensions under a Floquet drive which provides for the third periodicity necessary for the Hopf map. We show that the Hopf invariant of the micromotion fully captures the non-trivial winding structure of the Floquet system. We find that upon varying the period of the drive, in combination with a flattening procedure, the Hopf characterization can be experimentally invoked to deduce the full set of Floquet topological invariants of the two-dimensional quantum system. We thus propose a feasible approach for measuring the winding numbers as linkings in the dynamical response of the system.

Model setting – We start from a generic two-band model in two dimensions,

$$\mathcal{H}(\mathbf{k}, t) = \mathbf{h}(\mathbf{k}, t) \cdot \boldsymbol{\sigma} \quad (1)$$

written in terms of the Pauli matrices $\boldsymbol{\sigma}$ and quasi-momenta \mathbf{k} . Upon driving the system periodically with period T , the time-evolution of the system is captured by the time-ordered operator $\mathcal{U}(\mathbf{k}, t) = \mathcal{T} \exp[-i \int_0^t \mathcal{H}(\mathbf{k}, t') dt']$. Evaluated stroboscopically, $\mathcal{U}(\mathbf{k}, T) = e^{-i\mathcal{H}_F(\mathbf{k})T}$, it defines the quasienergy spectrum of the system through the time-independent Floquet Hamiltonian \mathcal{H}_F with eigenvalues ε_n for the two bands $n = 1, 2$. Due to the periodic nature of the Floquet spectrum, quasienergies can only be defined modulo 2π and can be restricted to the Floquet Brillouin Zone (FBZ), $-\pi/T < \varepsilon_n \leq \pi/T$. We label the two gaps which are centered around the quasienergy g/T by $g = 0$ and $g = \pi$. Since the quasienergy spectrum is defined on a circle, it is possible to obtain anomalous edge states lying at the π -gap connecting the bands through the FBZ edge.

This renders the equilibrium topological classification in terms of Chern number C_n inept to characterize driven systems (see Fig. 1). Instead, one needs to consider winding numbers, W_g , which are topological invariants associated with gaps rather than individual bands [13, 14].

The time evolution operator can be decomposed into two parts,

$$\mathcal{U}(\mathbf{k}, t) = \mathcal{U}_F(\mathbf{k}, t) e^{-i\mathcal{H}_F(\mathbf{k})t}, \quad (2)$$

corresponding to the effective Floquet Hamiltonian \mathcal{H}_F dictating the stroboscopic evolution at the end of a period T , and the time-periodic micromotion operator \mathcal{U}_F capturing the details within a period, whose stroboscopic effect equals the identity $\mathcal{U}_F(T) = \mathbf{1}$. In the high-frequency regime where the compactness of the FBZ becomes irrelevant, the micromotion describes only trivial corrections and we can focus on the evolution captured by the Floquet Hamiltonian. However, the overall effect of the micromotion can be non-trivial at lower frequencies by winding through the FBZ [14], giving rise to non-zero values for the winding number W_π .

For concreteness, we consider a two-dimensional honeycomb lattice with an energy offset Δ between sublattices A and B , and focus on a step-wise periodic drive [13, 39]. Driving is introduced by dividing one period into three stages of equal length $T/3$ during which the tunneling parameters are switched on and off in a cyclic manner. The tight-binding Hamiltonian in the momentum-space can be written as

$$\mathcal{H}(\mathbf{k}, t) = - \sum_{i=1}^3 J_i(t) \{ \cos(\mathbf{k} \cdot \mathbf{b}_i) \sigma_x + \sin(\mathbf{k} \cdot \mathbf{b}_i) \sigma_y \} + \frac{\Delta}{2} \sigma_z, \quad (3)$$

where the nearest-neighbor tunneling amplitudes J_i are along the directions $\mathbf{b}_1 = (-1, 0)$, $\mathbf{b}_2 = (\sqrt{3}/2, 1/2)$ and $\mathbf{b}_3 = (-\sqrt{3}/2, 1/2)$ in units of the nearest-neighbor distance. During the i^{th} stage within a period, only the hopping along the \mathbf{b}_i direction is allowed with an amplitude $J_i = J$ while the hopping amplitudes along the other two directions are set to zero. We note, however, that we obtain equivalent results for a (continuous) circularly-driven honeycomb lattice. The former has the advantage of theoretical simplicity whereas the latter has been already implemented in cold-atom experiments [17, 23, 25]. Even though such step-wise drives were initially introduced to demonstrate the topological distinction of non-equilibrium periodically driven systems, they have been already realized in photonic wave guides and their implementation in cold atoms is also possible [39].

The cyclic nature of the allowed tunneling directions breaks time-reversal symmetry and may induce chiral edge states in the quasienergy gaps g . Fig. 1 demonstrates the three possible combinations of edge states for an armchair-terminated strip with momentum k_\parallel along the periodic direction. Particularly, as can be seen in

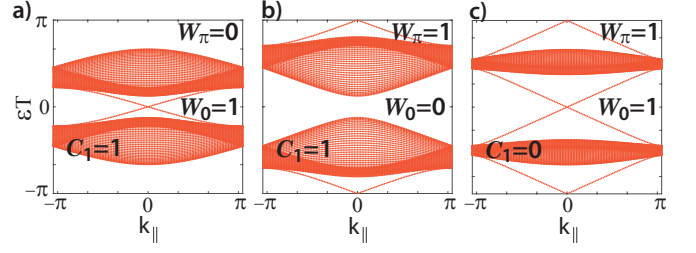


FIG. 1. Quasienergy spectrum of a step-wise drive introduced in Eq.(3) in a strip geometry for momentum k_\parallel along the periodic direction. Three different combinations of edge states appear in the 0 and/or the π -gap for a) $T = 2\pi/3J$, $\Delta = 0$; b) $T = 2\pi/2J$, $\Delta = 1.3J$ and c) $T = 2\pi/1.5J$, $\Delta = 0.1J$.

Fig. 1(c), the anomalous edge states appearing at the edge of the FBZ result in the break-down of the conventional bulk-boundary correspondence of static systems [40–44]. Instead, the bulk-boundary correspondence of Floquet systems is captured by the winding number W_g that account for the winding structure of the micromotion in contrast to the Chern number that can be associated to the effective Floquet Hamiltonian.

We now turn to the topological aspects alluded to above. We consider the evolution of a topologically trivial state $\Psi(\mathbf{k}, t = 0)$ under the effect of a time-periodic Hamiltonian (3) throughout an entire period $0 < t \leq T$. In two spatial dimensions, the quasimomentum \mathbf{k} defines a two-dimensional torus T^2 . Under the micromotion \mathcal{U}_F of the drive, the state returns to itself at the end of a period, $\Psi(\mathbf{k}, T) = \mathcal{U}_F(\mathbf{k}, T)\Psi(\mathbf{k}, 0) = \Psi(\mathbf{k}, 0)$, making the evolution periodic and defining a three-torus T^3 in $\mathbf{p} \equiv (k_x, k_y, t)$ -space. It is this periodicity in all three parameters that allows for establishing the topological characterization of the periodically driven system in terms of a Hopf map, which pertains to a map from S^3 to S^2 and arises by virtue of $\pi_3(S^2) = \mathbf{Z}$ [45, 46]. Mathematically, it can be generalized to T^3 by use of a composition map from T^3 to S^3 . This restrains the map to have values in a finite group $\mathbf{Z}_{2GDC(C_x, C_y, C_t)}$ in terms of the greatest common divisor of the Chern numbers C_i of the respective two-torus submanifolds within the three-dimensional torus formed by \mathbf{p} . Assuming these ‘weak invariants’ to be absent then renders the usual \mathbf{Z} -valued characterization. Specifically, the micromotion defines an evolution on the Bloch sphere S^2 , whose topology is described by the Hopf map conventionally given as

$$H = -\frac{1}{16\pi^2} \int A \wedge B,$$

where $A_i = -2i\Psi^\dagger \partial_i \Psi$ is the connection one form and $B = dA = \frac{1}{2} B_{ij} dp^i \wedge dp^j$, with $B_{ij} = -2i(\partial_i \Psi^\dagger \partial_j \Psi - \partial_j \Psi^\dagger \partial_i \Psi)$, entails the Hopf curvature two form. We can cast this Hopf invariant into a more practical form [47]

$$H = -\frac{1}{4\pi^2} \int d^3p \epsilon^{ijk} \Psi^\dagger \partial_i \Psi \partial_j \Psi^\dagger \partial_k \Psi, \quad (4)$$

which we shall use in the following.

Under the Hopf map, the trajectories followed by the inverse images of any two vectors on S^2 elucidate the topological invariant as a linking number L in T^3 . That is, the pre-images define linking circles and lines in the case of a non-trivial Hopf characterization. This correspondence has been previously employed to measure the Chern number of the Floquet bands in stroboscopic measurements [17]. Here, we show that the linking number of the micromotion provides direct access also to the winding number of Floquet topological insulators and, hence, captures the full topological classification of the periodically driven system. Moreover, we will propose how to measure this linking number in a quantum gas experiment.

We emphasize the crucial role of the periodicity in the system. The three-dimensional torus is formed by the micromotion, under the evolution of which the state has to be mapped onto itself at the end of a period. That is, the micromotion has to be isolated from the stroboscopic evolution by smoothly deforming the drive to obtain $\mathcal{U}(T) = \mathcal{U}_F(T) = \mathbb{1}$, i.e. degenerate quasienergy bands. This can be achieved by multiplying Eq.(2) with $e^{i\mathcal{H}_F T}$ from the right. However, there is an ambiguity in determining the effective Floquet Hamiltonian $\mathcal{H}_F^g(\mathbf{k}) = i \log \mathcal{U}(\mathbf{k}, T)/T$ when choosing different branches of the logarithm lying at gap $\pi - g$. As shown in Ref. [14], the micromotion operator associated with a chosen Hamiltonian can be implemented by evolving the system with $-\mathcal{H}_F^g$ for an amount of time T after completing one period of the drive,

$$\mathcal{U}_F^g(\mathbf{k}, t) = \begin{cases} \mathcal{U}(\mathbf{k}, t), & 0 < t \leq T, \\ e^{-i\mathcal{H}_F^g(\mathbf{k})(T-t)}, & T < t \leq 2T, \end{cases} \quad (5)$$

with a rescaling of the period. Physically, this corresponds to contracting the bands ($\mathcal{U}(T) = \mathbb{1}$) into degeneracy at the center or at the edge of the FBZ. Applying \mathcal{U}_F^g to a topologically trivial initial state, this state acquires the periodicity of the micromotion, thereby naturally tracing an evolution of the well-defined Bloch vector as function of the variables on T^3 governed by the Hopf map. Consequently, the driven system is described by two Hopf constructions, hence, by two Hopf invariants H_g depending on whether the branch cut is taken along π or 0. The former reveals the topology of the Hopf map at the π -gap as the micromotion winds the state through the zone edge, whereas the latter corresponds to the Hopf invariant at the zero gap.

As one of our main results, we find that our viewpoint naturally encloses the previously found topological characterizations by connecting to the winding number pertaining to the gap selected by the branch cut. Indeed, by writing the evolution operators in the basis of Bloch vectors, we analytically calculate that the winding

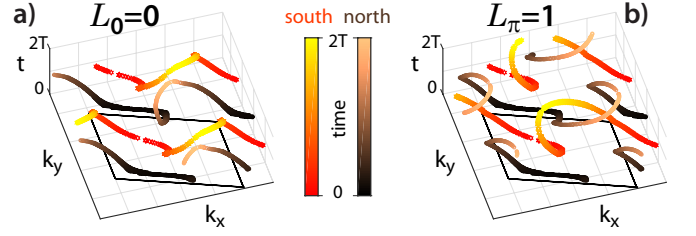


FIG. 2. Numerical calculation of the linking number L_g associated to each quasienergy gap of Fig. 1(b). A state evolving under the periodic drive (5) visits the north and the south poles of the Bloch sphere before returning to its original position at $t = 2T$, where the time is encoded in the color gradient. Inverse images of the poles draw trajectories which (a) do not link at the central gap $g = 0$ and (b) link once within the momentum-space BZ marked by the parallelogram at the $g = \pi$ -gap.

number [13, 14],

$$W_g = \int \frac{d^3p}{24\pi^2} \varepsilon^{ijk} \text{Tr}[(\mathcal{U}_F^{g\dagger} \partial_i \mathcal{U}_F^g F)(\mathcal{U}_F^{g\dagger} \partial_j \mathcal{U}_F^g)(\mathcal{U}_F^{g\dagger} \partial_k \mathcal{U}_F^g)], \quad (6)$$

directly coincides with the Hopf characterization [48]

$$H_g = W_g. \quad (7)$$

Moreover, the difference between these two Hopf invariants gives the Chern number of the quasienergy bands.

To make these statements concrete, we can revert to the explicit values of these topological invariants in the setting of our illustrative model. We numerically calculate the Hopf invariants (winding numbers) given in Fig. 1 which can be directly observed as a linking number, ($H_g = L_g$), in the evolution of a state in three-dimensional \mathbf{p} -space. Fig. 2 demonstrates the parameter space explored by the inverse images of the north and south poles of the Bloch sphere, when the periodic drive is suddenly switched on with the parameters given in Fig. 1(b). Upon employing the return map, when we choose the branch cut for which the quasienergy bands are degenerate at the FBZ edge, the trajectories in Fig. 2(a) do not link, corresponding to the vanishing winding number at the 0-gap, $L_0 = W_0 = 0$. However, when the quasienergy bands are contracted into degeneracy at the FBZ center, the quasienergy spectrum features edge states winding through the edge of the FBZ. Correspondingly, the trajectories in Fig. 2(b) link once, giving $L_\pi = W_\pi = 1$.

Experimental Scheme – We now turn to the experimental implications of our characterization. The trajectories depicted in Fig. 2 can be measured experimentally in optical lattices via the state-tomography technique [23, 49] where the inverse images of the poles appear as vortices in the azimuthal Bloch-sphere angle of the time-evolved state $\Psi(\mathbf{k}, t)$ as a function of \mathbf{k} . This

method has been recently employed in a circularly driven honeycomb lattice to measure the Chern number with great precision [17]. To reveal the Chern number of the bands, the evolution of the singularities must be monitored stroboscopically as it is done in the experiment. However, since the Chern numbers of the two bands, $C_1 = -C_2$, are given by the difference of the winding numbers above and below a band,

$$C_n = (-1)^n (W_\pi - W_0), \quad (8)$$

this measurement is not enough to reveal the full topological characterization of a Floquet system. Therefore, here we propose a different scheme that relies on tracing the evolution within one period $0 < t \leq T$. Measurement of the linking number requires the isolation of the micromotion from the stroboscopic dynamics to be able to observe $\mathcal{U}_F^g(T) = \mathbb{1}$. In principle, this can be achieved by designing the return map depicted in Eq. (5). However in practice, it is not possible to engineer \mathcal{H}_F^g as static Hamiltonian. Alternatively, here we propose a more elegant and feasible approach to extract the micromotion in the experiments directly.

Our scheme relies on the particle-hole symmetry of the Hamiltonian and on folding the quasienergy spectrum. Namely, when the drive is monitored in terms of a doubled $\tilde{T} = 2T$ (with respect to which it is, obviously, also periodic), the quasienergy bands fold once around the energy $\varepsilon = \pm\pi/2T$. As a result, the edge states at the π -gap of the original drive lie at the zero-gap of the new quasienergy spectrum of period $2T$. This also implies that the winding number in the zero-gap of the folded Floquet spectrum is given by the sum of the two winding numbers of the original drive of period T ; i.e. $\tilde{W}_0^{(2T)} = W_0^{(T)} + W_\pi^{(T)}$. Taking power from this observation, we now focus on making the quasienergy bands flat at the quarter of the FBZ, $\varepsilon = \pm\pi/2T$, as depicted in Fig. 3 so that they become degenerate when the period is doubled.

In principle, by slightly deforming any drive, the quasienergy bands can be adiabatically flattened as in Fig. 3(a), which is topologically identical to the Floquet spectrum given Fig. 1(c). This can be achieved by tuning the driving frequency ω (see e.g. Ref. [15]) individually at each quasimomentum \mathbf{k} (in repeated experiments) to shift the quasienergies within the FBZ. We identify this modified drive with a tilde, e.g. $\tilde{\mathcal{H}}(\mathbf{k}, t)$, as well as its topological invariants. In practice, the deformation needs to be performed only at a given number of points in the BZ enough to reveal the trajectories of the vortices. Moreover, this experimental implementation does not require the knowledge of the theoretical model, since the \mathbf{k} -dependent quasienergy gap can be found experimentally from the stroboscopic evolution after quenches [15]).

Once the quasienergies are flattened, the time evolution operator over a double period becomes the identity,

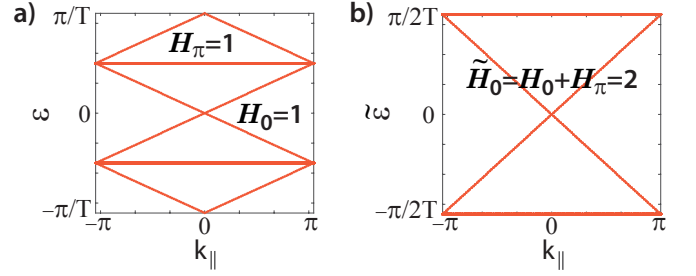


FIG. 3. Folding of the quasienergy spectrum when the period is doubled. The Hopf invariant of the central gap over the double period $\tilde{T} = 2T$ is the sum of the topological invariants of the both gaps of the original drive, $\tilde{H}_0 = H_0 + H_\pi$, which can be directly revealed as the linking number.

$\tilde{\mathcal{U}}(2T) = \mathbb{1}$, directly corresponding to the micromotion operator $\tilde{\mathcal{U}}_F^0(2T)$. Fig. 3(b) demonstrates the degenerate Floquet spectrum over the doubled period where the linking number corresponds to the winding number at the zero-gap, $\tilde{L}^{(2T)} = \tilde{W}_0^{(2T)} = 2$. This linking number can be measured via state-tomography by tracing the time evolution of the state throughout $0 < t \leq 2T$. In terms of the winding numbers of the original Hamiltonian, this corresponds to their sum,

$$\tilde{L}^{(2T)} = W_0^{(T)} + W_\pi^{(T)}, \quad (9)$$

which is, on its own, still not enough to identify the winding numbers individually. The missing information can be acquired by combining the equations (8) which can be obtained via a stroboscopic measurement and (9) of the micromotion [17].

Conclusion and Discussion – We have shown that two-dimensional Floquet topological insulators with two bands are characterized by two Hopf constructions rooted in the inherent periodicity of micromotion. The associated Hopf invariants are found to directly correspond to previously described winding numbers and, thus, provide a complete topological characterization of the system. The attained perspective is not only appealing from a theoretical point of view, employing Hopf invariants to describe the quasienergy band topology, but also intimately relates to experimental setups, bringing these deep notions within experimental reach. Indeed, by proposing a viable band folding scheme, this physics is directly measurable in cold atomic systems.

Finally, we point out a peculiarity compared to static systems [34, 36, 37]. In three dimensions, Hopf insulators produce a \mathbf{Z} invariant, stemming from the fact that the Hopf map coincides with the target space spanned by two-band models. This invariant is not present in the tenfold periodic table, as K-theory allows for a trivial addition of bands. Note that this invariant also arises when all three Chern numbers of the underlying cuts (T^2) are zero. In contrast, when a two-dimensional system is driven, the third periodicity arises by virtue of

time translations. The periodic table for Floquet states [12], predicts a $\mathbf{Z}^{\times n}$ classification, where n refers to the number of gaps, showing e.g. that there is a 0- and π -gap topological invariant for the case of two bands. As we have demonstrated, these numbers directly coincide with our framework and the Hopf characterization upon the flattening procedure, highlighting the difference between $(2+1)$ -dimensional Floquet states and 3 dimensional static insulators, as also already alluded to by the difference in periodic tables themselves. This gives incentive to speculate that our approach can be generalized to describe the topology of any desired pair of bands in a general two-dimensional class A Floquet insulator. In this regard we remark that in specific scenarios the Hopf maps can be obtained by considering stacks of Chern insulators or their non-trivial winding within the Brillouin zone [34, 35, 45, 46]. This therefore poses the question whether the Chern number of quasienergy bands can be phrased into such a “stacking” perspective in the time direction, using e.g. a Hopf map that is the composition of the Hopf maps for both gaps. Indeed, from our construction it directly follows that restrictions on the Hopf invariant correspond to Chern numbers of cuts and vice versa. Finally, this also stimulates connections to Topological Hopf-Chern insulators [35], which will in turn relate to the many-band generalization.

Acknowledgments – F.N.Ü and A.E. acknowledge the support from the Deutsche Forschungsgemeinschaft (DFG) via the Research Unit FOR 2414 (under Project No. 277974659) and fruitful discussions with Christof Weitenberg. R.-J.S gratefully acknowledges funding via Ashvin Vishwanath from the Center for the Advancement of Topological Materials initiative, an Energy Frontier Research Center funded by the U.S. Department of Energy, Office of Science.

Note added – While finalizing this work, we became aware of the insightful work by Schuster et al. [50] which, in contrast to the present paper, considers the Floquet driving of an underlying three-dimensional Hopf insulator. Such systems were shown to have an additional \mathbf{Z}_2 invariant associated with the Witten anomaly.

* unal@pks.mpg.de

† eckardt@pks.mpg.de

‡ robertjanslager@fas.harvard.edu

- [1] M. Z. Hasan and C. L. Kane, “Colloquium: Topological insulators,” *Rev. Mod. Phys.* **82**, 3045–3067 (2010).
- [2] Xiao-Liang Qi and Shou-Cheng Zhang, “Topological insulators and superconductors,” *Rev. Mod. Phys.* **83**, 1057–1110 (2011).
- [3] Alexei Kitaev, “Periodic table for topological insulators and superconductors,” (AIP, 2009) pp. 22–30.
- [4] Shinsei Ryu, Andreas P Schnyder, Akira Furusaki, and Andreas WW Ludwig, “Topological insulators and superconductors: tenfold way and dimensional hierarchy,”

New Journal of Physics **12**, 065010 (2010).

- [5] Liang Fu, “Topological crystalline insulators,” *Phys. Rev. Lett.* **106**, 106802 (2011).
- [6] Robert-Jan Slager, Andrej Mesaros, Vladimir Juričić, and Jan Zaanen, “The space group classification of topological band-insulators,” *Nature Physics* **9**, 98 (2012).
- [7] Jorrit Kruthoff, Jan de Boer, Jasper van Wezel, Charles L. Kane, and Robert-Jan Slager, “Topological classification of crystalline insulators through band structure combinatorics,” *Phys. Rev. X* **7**, 041069 (2017).
- [8] Hoi Chun Po, Ashvin Vishwanath, and Haruki Watanabe, “Symmetry-based indicators of band topology in the 230 space groups,” *Nature Communications* **8**, 50 (2017).
- [9] J. Höller and A. Alexandradinata, “Topological Bloch oscillations,” *Phys. Rev. B* **98**, 024310 (2018).
- [10] Adrien Bouhon, Annica M Black-Schaffer, and Robert-Jan Slager, “Wilson loop approach to topological crystalline insulators with time reversal symmetry,” arXiv preprint arXiv:1804.09719 (2018).
- [11] Barry Bradlyn, L. Elcoro, Jennifer Cano, M. G. Vergniory, Zhijun Wang, C. Felser, M. I. Aroyo, and B. Andrei Bernevig, “Topological quantum chemistry,” *Nature* **547**, 298 (2017).
- [12] Rahul Roy and Fenner Harper, “Periodic table for Floquet topological insulators,” *Phys. Rev. B* **96**, 155118 (2017).
- [13] Takuya Kitagawa, Erez Berg, Mark Rudner, and Eugene Demler, “Topological characterization of periodically driven quantum systems,” *Phys. Rev. B* **82**, 235114 (2010).
- [14] Mark S. Rudner, Netanel H. Lindner, Erez Berg, and Michael Levin, “Anomalous edge states and the bulk-edge correspondence for periodically driven two-dimensional systems,” *Phys. Rev. X* **3**, 031005 (2013).
- [15] F. Nur Ünal, Babak Seradjeh, and Andre Eckardt, “How to directly measure Floquet topological invariants in optical lattices,” arXiv:1812.04636 (2018).
- [16] Ce Wang, Pengfei Zhang, Xin Chen, Jinlong Yu, and Hui Zhai, “Scheme to measure the topological number of a Chern insulator from quench dynamics,” *Phys. Rev. Lett.* **118**, 185701 (2017).
- [17] Matthias Tarnowski, F Nur Ünal, Nick Fläschner, Benno S Rem, André Eckardt, Klaus Sengstock, and Christof Weitenberg, “Characterizing topology by dynamics: Chern number from linking number,” arXiv:1709.01046 (2017).
- [18] Wei Sun, Chang-Rui Yi, Bao-Zong Wang, Wei-Wei Zhang, Barry C. Sanders, Xiao-Tian Xu, Zong-Yao Wang, Joerg Schmiedmayer, Youjin Deng, Xiong-Jun Liu, Shuai Chen, and Jian-Wei Pan, “Uncover topology by quantum quench dynamics,” *Phys. Rev. Lett.* **121**, 250403 (2018).
- [19] Jinlong Yu, “Phase vortices of the quenched Haldane model,” *Phys. Rev. A* **96**, 023601 (2017).
- [20] X-X Yuan, L He, S-T Wang, D-L Deng, F Wang, W-Q Lian, X Wang, C-H Zhang, H-L Zhang, X-Y Chang, et al., “Observation of topological links associated with Hopf insulators in a solid-state quantum simulator,” *Chinese Physics Letters* **34**, 060302 (2017).
- [21] Tracy Li, Lucia Duca, Martin Reitter, Fabian Grusdt, Eugene Demler, Manuel Endres, Monika Schleier-Smith, Immanuel Bloch, and Ulrich Schneider, “Bloch state tomography using Wilson lines,” *Science* **352**, 1094–1097

- (2016).
- [22] Monika Aidelsburger, Michael Lohse, C Schweizer, Marcos Atala, Julio T Barreiro, S Nascimbene, NR Cooper, Immanuel Bloch, and N Goldman, “Measuring the Chern number of Hofstadter bands with ultracold bosonic atoms,” *Nat. Phys.* **11**, 162–166 (2015).
 - [23] N. Fläschner, D Vogel, M. Tarnowski, B. S. Rem, D.-S. Lühmann, M. Heyl, J. C. Budich, L. Mathey, K. Sengstock, and C. Weitenberg, “Observation of dynamical vortices after quenches in a system with topology,” *Nat. Phys.* **14**, 265 (2018).
 - [24] N. Fläschner, B. S. Rem, M. Tarnowski, D. Vogel, D.-S. Lühmann, K. Sengstock, and C. Weitenberg, “Experimental reconstruction of the berry curvature in a Floquet Bloch band,” *Science* **352**, 1091–1094 (2016).
 - [25] Gregor Jotzu, Michael Messer, Rémi Desbuquois, Martin Lebrat, Thomas Uehlinger, Daniel Greif, and Tilman Esslinger, “Experimental realization of the topological Haldane model with ultracold fermions,” *Nature* **515**, 237 (2014).
 - [26] M. Aidelsburger, M. Atala, M. Lohse, J. T. Barreiro, B. Paredes, and I. Bloch, “Realization of the Hofstadter hamiltonian with ultracold atoms in optical lattices,” *Phys. Rev. Lett.* **111**, 185301 (2013).
 - [27] Hirokazu Miyake, Georgios A. Siviloglou, Colin J. Kennedy, William Cody Burton, and Wolfgang Ketterle, “Realizing the Harper Hamiltonian with laser-assisted tunneling in optical lattices,” *Phys. Rev. Lett.* **111**, 185302 (2013).
 - [28] André Eckardt, “Colloquium: Atomic quantum gases in periodically driven optical lattices,” *Rev. Mod. Phys.* **89**, 011004 (2017).
 - [29] Wenchao Hu, Jason C. Pillay, Kan Wu, Michael Pasek, Perry Ping Shum, and Y. D. Chong, “Measurement of a topological edge invariant in a microwave network,” *Phys. Rev. X* **5**, 011012 (2015).
 - [30] Fei Gao, Zhen Gao, Xihang Shi, Zhaoju Yang, Xiao Lin, Hongyi Xu, John D. Joannopoulos, Marin Soljačić, Hongsheng Chen, Ling Lu, and et al., “Probing topological protection using a designer surface plasmon structure,” *Nat. Commun.* **7** (2016), 10.1038/ncomms11619.
 - [31] Seababrat Mukherjee, Alexander Spracklen, Manuel Valiente, Erika Andersson, Patrik hberg, Nathan Goldman, and Robert R Thomson, “Experimental observation of anomalous topological edge modes in a slowly driven photonic lattice,” *Nat. Commun.* **8** (2017), 10.1038/ncomms13918.
 - [32] Seababrat Mukherjee, Harikumar K. Chandrasekharan, Patrik hberg, Nathan Goldman, and Robert R Thomson, “State-recycling and time-resolved imaging in topological photonic lattices,” *Nature Commun.* **9** (2018), 10.1038/s41467-018-06723-y.
 - [33] Lukas J. Maczewsky, Julia M. Zeuner, Stefan Nolte, and Alexander Szameit, “Observation of photonic anomalous Floquet topological insulators,” *Nat. Commun.* **8** (2017), 10.1038/ncomms13756.
 - [34] Chunxiao Liu, Farzan Vafa, and Cenke Xu, “Symmetry-protected topological hopf insulator and its generalizations,” *Phys. Rev. B* **95**, 161116 (2017).
 - [35] Ricardo Kennedy, “Topological Hopf-Chern insulators and the Hopf superconductor,” *Phys. Rev. B* **94**, 035137 (2016).
 - [36] D.-L. Deng, S.-T. Wang, C. Shen, and L.-M. Duan, “Hopf insulators and their topologically protected surface states,” *Phys. Rev. B* **88**, 201105 (2013).
 - [37] Joel E. Moore, Ying Ran, and Xiao-Gang Wen, “Topological surface states in three-dimensional magnetic insulators,” *Phys. Rev. Lett.* **101**, 186805 (2008).
 - [38] Thomas Schuster, Felix Flicker, Ming Li, Svetlana Kotochigova, Joel E. Moore, Jun Ye, and Norman Y. Yao, “Realizing Hopf Insulators in Dipolar Spin Systems,” arXiv e-prints, arXiv:1901.08597 (2019), arXiv:1901.08597 [cond-mat.quant-gas].
 - [39] A. Quelle, C. Weitenberg, K. Sengstock, and C. Morais-Smith, “Driving protocol for a Floquet topological phase without static counterpart,” *New J. Phys.* **19** (2017).
 - [40] Robert-Jan Slager, Louk Rademaker, Jan Zaanen, and Leon Balents, “Impurity-bound states and Green’s function zeros as local signatures of topology,” *Phys. Rev. B* **92**, 085126 (2015).
 - [41] Yasuhiro Hatsugai, “Chern number and edge states in the integer quantum Hall effect,” *Phys. Rev. Lett.* **71**, 3697–3700 (1993).
 - [42] Robert-Jan Slager, Vladimir Juričić, Ville Lahtinen, and Jan Zaanen, “Self-organized pseudo-graphene on grain boundaries in topological band insulators,” *Phys. Rev. B* **93**, 245406 (2016).
 - [43] Andrew M. Essin and Victor Gurarie, “Bulk-boundary correspondence of topological insulators from their respective Green’s functions,” *Phys. Rev. B* **84**, 125132 (2011).
 - [44] Jun-Won Rhim, Jens H. Bardarson, and Robert-Jan Slager, “Unified bulk-boundary correspondence for band insulators,” *Phys. Rev. B* **97**, 115143 (2018).
 - [45] L.S. Pontrjagin, *Mat. Sbornik (Recueil Mathématique NS)* **9**, 331 (1941).
 - [46] Yu G Makhlin and T Sh Misirpashaev, “Topology of vortex-soliton intersection: invariants and torus homotopy,” *JETP Lett.* **61**, 49–49 (1995).
 - [47] Ji-rong Ren, Ran Li, and Yi-shi Duan, “Inner topological structure of Hopf invariant,” *J.Math. Phys.* **48**, 073502 (2007).
 - [48] See supplementary for details.
 - [49] Philipp Hauke, Maciej Lewenstein, and André Eckardt, “Tomography of band insulators from quench dynamics,” *Phys. Rev. Lett.* **113**, 045303 (2014).
 - [50] Thomas Schuster, Snir Gazit, Joel E. Moore, and Norman Y. Yao, “Floquet Hopf Insulators,” arXiv e-prints, arXiv:1903.02558 (2019), arXiv:1903.02558 [cond-mat.mes-hall].

Supplementary for “Hopf characterization of two-dimensional Floquet topological insulators”

In this supplementary, we analytically prove that the Hopf invariant given in Eq. (4) of the main text is equal to the winding number previously studied in the literature. For this purpose, we start by contracting the winding number given in Eq. (6) into the form

$$W = -\frac{1}{24\pi^2} \int d^3p \varepsilon^{ijk} \text{Tr}[U^\dagger \partial_i U \cdot \partial_j U^\dagger \cdot \partial_k U], \quad (\text{S1})$$

by using the unitarity of the evolution operator, $UU^\dagger = 1$ and $\partial_i U \cdot U^\dagger + U \partial_{ji} U^\dagger = 0$. Following the Einstein notation, the trace can be written as

$$W = -\frac{1}{24\pi^2} \int d^3p \varepsilon^{ijk} \sum_{a,b,c,d} U_{ab}^\dagger \partial_i U_{bc} \partial_j U_{cd}^\dagger \partial_k U_{da}, \quad (\text{S2})$$

where the indices $a, b, c, d = 1, 2$ scan the space formed by the two bands. Matrix elements of the evolution operator can be found by evolving an initial state $|\psi_a\rangle$ which we take to be \mathbf{k} -independent, $U_{ab}(\mathbf{k}, t) = \langle \psi_a | U(\mathbf{k}, t) | \psi_b \rangle$. The derivatives act only on the time-evolved state which we denote as $|\Psi_a(\mathbf{k}, t)\rangle = U(\mathbf{k}, t) |\psi_b\rangle$,

$$\begin{aligned} W &= -\frac{1}{24\pi^2} \int d^3p \varepsilon^{ijk} \sum_{a,b,c,d} \langle \Psi_a(\mathbf{k}, t) | \psi_b \rangle \partial_i \langle \psi_b | \Psi_c(\mathbf{k}, t) \rangle \partial_j \langle \Psi_c(\mathbf{k}, t) | \psi_d \rangle \partial_k \langle \psi_d | \Psi_a(\mathbf{k}, t) \rangle, \\ &= -\frac{1}{24\pi^2} \int d^3p \varepsilon^{ijk} \sum_{a,c} \langle \Psi_a(\mathbf{k}, t) | \partial_i \Psi_c(\mathbf{k}, t) \rangle \langle \partial_j \Psi_c(\mathbf{k}, t) | \partial_k \Psi_a(\mathbf{k}, t) \rangle. \end{aligned} \quad (\text{S3})$$

Here, we dropped the terms equal to identity $\sum_a |\psi_a\rangle \langle \psi_a| = \mathbb{1}$. Therefore, we identify the four terms giving contribution to the winding numbers as,

$$W = -\frac{1}{24\pi^2} \int d^3p \varepsilon^{ijk} \left[\underbrace{\Psi_1^\dagger \partial_i \Psi_1 \partial_j \Psi_1^\dagger \partial_k \Psi_1}_{W_1} + \underbrace{\Psi_1^\dagger \partial_i \Psi_2 \partial_j \Psi_2^\dagger \partial_k \Psi_1}_{W_2} + \underbrace{\Psi_2^\dagger \partial_i \Psi_1 \partial_j \Psi_1^\dagger \partial_k \Psi_2}_{W_3} + \underbrace{\Psi_2^\dagger \partial_i \Psi_2 \partial_j \Psi_2^\dagger \partial_k \Psi_2}_{W_4} \right]. \quad (\text{S4})$$

One can intuitively see that $W_1 = W_4$ and $W_2 = W_3$ by using symmetry arguments but we also prove it below. The important point is to relate the mixed term W_2 to the first term W_1 which is already in the same form as the Hopf invariant Eq.(4).

The time-evolved wave functions $\Psi_a(\mathbf{k}, t)$ are two-component normalized spinors on the Bloch sphere. They can be written in terms of two complex scalar fields $z_1(\mathbf{k}, t)$ and $z_2(\mathbf{k}, t)$ as $\Psi_1(\mathbf{k}, t) = (z_1(\mathbf{k}, t), z_2(\mathbf{k}, t))^T$ and $\Psi_2(\mathbf{k}, t) = (-z_2(\mathbf{k}, t), z_1(\mathbf{k}, t))^T$, satisfying the normalization condition $|z_1(\mathbf{k}, t)|^2 + |z_2(\mathbf{k}, t)|^2 = 1$ at each \mathbf{k} and t . We insert these forms into the first term in Eq. (S4),

$$\begin{aligned} W_1 &= (z_1, z_2)(\partial_i z_1, \partial_i z_2)^T (\partial_j z_1, \partial_j z_2)(\partial_k z_1, \partial_k z_2)^T \\ &= z_1^* \partial_i z_1 \partial_j z_1^* \partial_k z_1 + z_1^* \partial_i z_1 \partial_j z_2^* \partial_k z_2 + z_2^* \partial_i z_2 \partial_j z_1^* \partial_k z_1 + z_2^* \partial_i z_2 \partial_j z_2^* \partial_k z_2 \\ &= z_1^* \partial_i z_1 \partial_j z_2^* \partial_k z_2 + z_2^* \partial_i z_2 \partial_j z_1^* \partial_k z_1, \end{aligned} \quad (\text{S5})$$

where the terms symmetric in ijk vanish because of the levi-civita operator in the integral, e.g. $z_1^* \partial_i z_1 \partial_j z_1^* \partial_k z_1 = -z_1^* \partial_k z_1 \partial_j z_1^* \partial_i z_1 = 0$. It can be directly seen that $W_1 = W_4$ when we write the W_4 term like

$$W_4 = z_2^* \partial_i z_2 \partial_j z_2^* \partial_k z_2 + z_2^* \partial_i z_2 \partial_j z_1^* \partial_k z_1 + z_1^* \partial_i z_1 \partial_j z_2^* \partial_k z_2 + z_1^* \partial_i z_1 \partial_j z_1^* \partial_k z_1 = W_1. \quad (\text{S6})$$

Similarly,

$$\begin{aligned} W_2 &= z_1^* \partial_i z_2^* \partial_j z_2 \partial_k z_1 - z_1^* \partial_i z_2^* \partial_j z_1 \partial_k z_2 - z_2^* \partial_i z_1^* \partial_j z_2 \partial_k z_1 + z_2^* \partial_i z_1^* \partial_j z_1 \partial_k z_2 \\ &= 2(z_1^* \partial_i z_1 \partial_j z_2^* \partial_k z_2 + z_2^* \partial_i z_2 \partial_j z_1^* \partial_k z_1) = 2W_1, \end{aligned} \quad (\text{S7})$$

where we again use the anti-symmetry of the levi-civita to swap the indices or the derivatives, e.g. $z_1^* \partial_i z_2^* \partial_j z_2 \partial_k z_1 = -z_1^* \partial_k z_2^* \partial_j z_2 \partial_i z_1 = z_1^* \partial_j z_2^* \partial_k z_2 \partial_i z_1$. We then prove that the contributions to the winding number (S4) coming from the band mixing terms are twice the contribution resulting from a single eigenstate, $W_2 = 2W_1$, so that

$W_1 + W_2 + W_3 + W_4 = 6W_1$. With this, we conclude our proof that the winding number is equal to the Hopf invariant,

$$W = -\frac{1}{4\pi^2} \int d^3p \, \varepsilon^{ijk} \, \Psi_1^\dagger \partial_i \Psi_1 \partial_j \Psi_1^\dagger \partial_k \Psi_1 = H. \quad (\text{S8})$$

Consequently, the periodically driven system can be topologically characterized in terms of a Hopf map where the Hopf invariant reveals the number of edge states in the quasienergy spectrum. Note that one can arrive at the same conclusion also through the approach followed by Schuster et al. in the supplementary of Ref. [50], by writing the evolution operator as $U(\mathbf{k}, t) = e^{i\phi(\mathbf{k}, t)} |\Psi(\mathbf{k}, t)\rangle \langle \Psi(\mathbf{k}, t)| + e^{-i\phi(\mathbf{k}, t)} (1 - |\Psi(\mathbf{k}, t)\rangle \langle \Psi(\mathbf{k}, t)|)$ where $\pm\phi(\mathbf{k}, t)$ are the phasebands for the two bands symmetric around zero due to the particle-hole symmetry.